Research Article

Magneto Jeffrey Nanofluid Bioconvection over a Rotating Vertical Cone due to Gyrotactic Microorganism

S. Saleem [ID],[1] **Hunza Rafiq,**[2] **A. Al-Qahtani,**[1] **Mohamed Abd El-Aziz** [ID]**,**[1,3] **M. Y. Malik,**[1] **and I. L. Animasaun** [ID]**** [4]

[1]*Department of Mathematics, College of Sciences, King Khalid University, Abha 61413, Saudi Arabia*
[2]*Department of Sciences and Humanities, National University of Computers and Emerging Sciences, Lahore 54000, Pakistan*
[3]*Department of Mathematics, Faculty of Science, Helwan University, Helwan, Cairo 11975, Egypt*
[4]*Department of Mathematical Sciences, Federal University of Technology, Akure, Nigeria*

Correspondence should be addressed to S. Saleem; saakhtar@kku.edu.sa

The particular inquiry is made to envision the behavioral characteristics of gyrotactic microorganism effects on the MHD flow of Jeffrey nanofluid. Together the nanoparticles and motile microorganism are inducted into the modeled nonlinear differential equations. The optimal solutions for the governing equations are tackled by optimal homotopy analysis method. The physical characteristics of the relatable parameters are explored and deliberated in terms of graphs and numerical charts. Also, the precision of the present findings is certified by equating them with the previously published work. It is explored that rescaled density of the motile microorganisms contracts with bioconvection Peclet number Pe. It is seen that bioconvection Rayleigh number Rb shrinks the magnitude of tangential velocity. Also, bioconvection Schmidt number Sb augments the reduced density number of the motile microorganisms.

1. Literature Survey

Non-Newtonian fluid mechanics is a subject which is essentially interdisciplinary in its nature and which is also wide in its area of application. Indeed, non-Newtonian behavior comes across mostly in organic and allied processing engineering. It is too useful in the excavating industry, where slurries and muds are controlled, and in applications like lubrication and biomedical flow phenomena. The imitation of nonlinear fluid flow occurrences is thus of significance to engineering. Everyday uses of specific flows are established in freezing progressions where a coolant is executed on continuously moving surface. Non-Newtonian fluids along heat and mass transfer are correspondingly crucial in food dispensation, heavy oils, and lubricants [1–5].

An important area of study is mixed convectional flows, which occurs in atmospheric boundary layer flows, heat exchangers, solar collectors, and nuclear reactors. It establishes in a condition wherever the impacts of buoyantic

forces due to forced convection turn to be considerable. In this existing effort, a cone is placed in a nonlinear fluid through the cone axis together with the outer flow is explored. Heat transfer analysis with combined convective flow about rotating cone-shaped tool is splendidly common in automobile and biochemical productions. Hering and Grosh [6] have conferred a variety of similarity solutions for cone shaped bodies in detail. Anilkumar and Roy [7] achieved the self-similar solutions for time dependent flow over a rotating cone. Nadeem and Saleem [8] deliberated a theoretical analysis for MHD flow above a spinning cone. The flow over conic shape objects has been studied by various investigators [9–12].

In emerging world, study of nanofluids has extended too much consideration by the investigators because of its features to improve the thermal conductivity relative to base fluids. It was suggested by Choi [13]. Nanofluids have been found to possess enhanced thermos-physical properties such as viscosity, thermal conductivity, thermal diffusivity, and

convective heat-transfer coefficients compared with those of base fluids like ethylene glycol, water, oil, etc. because of these enhanced properties nanofluids are used in several electronic applications (cooling of microchips, fluidic digital display devices, micro-electromechanical systems, micro-reactors, etc.), pharmaceutical processes, transportation industry, in biomedical (nano-drug delivery, cancer therapeutics, cryopreservation, nano-cryosurgery, sensing and imaging, etc.) and many others. Buongiorno [14] and Kakaç and Pramuanjaroenkij [15] have inspected an inclusive review of convective transporting nanofluids. Effects of CuO nanoparticles on heat transfer behavior of PCM in solidification process considering radiative source term were explored by Sheikholeslami et al. [16]. A number of investigational and hypothetical mechanisms connected to nanofluids are specified in [17–21].

The investigational and hypothetical analysis of the magnetohydrodynamic flows is significant from the scientific point of view, since it has countless worthy applications like magnetohydrodynamic electrical power generation, geophysics, etc. Scientifically, this occurrence is stated in the configuration of renowned Navier-Stokes equations in combination with Maxwell equations. Rashidi et al. [22] deliberated the study of the second law of thermodynamics functional to incompressible nanofluid flowing above a permeable rotational disk under vertical magnetic field. Ellahi [23] observed the flow features of MHD fluid with temperature-dependent viscosity. Awais et al. [24] worked on MHD Sisko fluid flow adjacent to the axisymmetric stagnation point near a stretching cylinder.

An important area of study is bioconvectional flows. Bioconvection [25] designs are generally perceived in the research workshop in narrow suspensions of arbitrarily, however on ordinary upwardly, swimming microorganisms which are a slight thicker than water and however have also been seen in situ in micro patches of zooplankton. Ahmed et al. [26] discussed the magnetohydrodynamic combined convective boundary-layer stagnation point flow of a nanofluid towards an elongating surface together with nanoparticles and gyrotactic microorganisms. Kuznetsov [27] explored the bioconvection in a horizontal layer occupied with a nanofluid. The idea was to use microorganisms to encourage or improve convection in a nanofluid. Khan and Makinde [28, 29] inspected effects of heat and mass transfer with bioconvection on a nanofluid flow. Raju and Sandeep [30] considered the thermal and mass flux activities of MHD bioconvection flow above two channels. Zaimi et al. [31] started a study of stagnation point flow to a stretching or shrinking plate in a nanofluid by gyrotactic microorganisms. Makinde and Sadia et al. [32] discussed phenomena of bioconvection in nanofluid containing gyrotactic microorganisms about a wavy cone. Makinde and Animasaun [33] investigated bioconvection nanofluid flow with nonlinear thermal radiation and quartic autocatalysis chemical reaction.

To the best of authors' information, the study associated with flow, heat, and mass transfer features of gyrotactic microorganisms containing MHD Jeffrey fluid over a vertical cone with nanoparticles has not been discovered so far. The extremely nonlinear differential equations of a Jeffrey nanofluid with prescribed heat and mass flux conditions
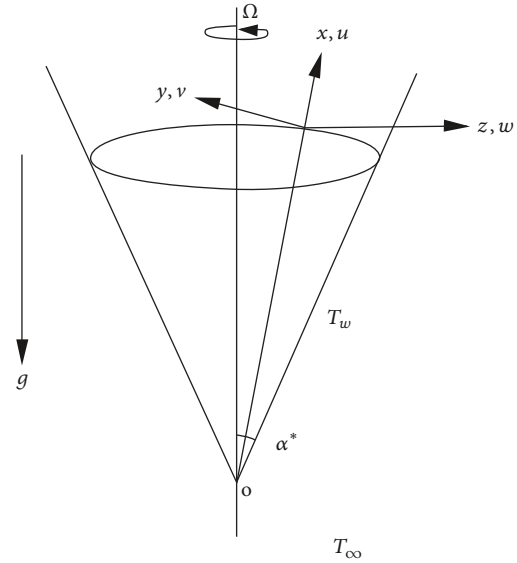

FIGURE 1: Geometry of the flow field.

are formerly elucidated by the optimal homotopy analysis method (OHAM) [34–40]. Likewise, the impact of appropriate parameters on the velocities, temperature, concentration fields, and gyrotactic microorganism are discovered and deliberated in detail through graphs and numerical tables. The precision of the analytical technique is also confirmed by comparing the results with the existing literature.

2. Mathematical Analysis

A time-dependent mixed convective boundary layer flow of Jeffrey nanofluid comprises gyrotactic microorganisms about a rotating cone. It is stated that the cone is in rotation with angular velocity Ω and creating unsteadiness in the flow field as displayed in Figure 1. The contribution of heat and mass flux is also reflected in the flow process. Further the flow is taken in MHD regime.

Flow analysis [7] is as follows:

$$x\frac{\partial u}{\partial x} + u + x\frac{\partial w}{\partial z} = 0, \tag{1}$$

$$\frac{\partial u}{\partial t} + u\frac{\partial u}{\partial x} + w\frac{\partial u}{\partial z} - \frac{v^2}{x} = \frac{v}{1+\lambda_1}\frac{\partial^2 u}{\partial z^2}$$

$$+ \frac{v\lambda_2}{1+\lambda_1}\left\{ u\frac{\partial^3 u}{\partial x \partial z^2} + \frac{\partial^2 u}{\partial z^2}\frac{\partial w}{\partial z} + \frac{\partial u}{\partial z}\frac{\partial^2 u}{\partial x \partial z} + w\frac{\partial^3 u}{\partial z^3}\right.$$

$$\left. + \frac{\partial^3 u}{\partial z^2 \partial t}\right\} - \frac{\sigma}{\rho}B^2 u \tag{2}$$

$$+ \left[(1 - C_\infty)\rho C_\infty \beta g \cos\alpha^* (T - T_\infty) - (\rho_p\right.$$

$$- \rho_{f\infty}) g (C - C_\infty)\cos\alpha^* - (n - n_\infty) g\gamma (\rho_m$$

$$\left. - \rho_{f\infty})\cos\alpha^*,\right.$$

$$\frac{\partial v}{\partial t} + u\frac{\partial v}{\partial x} + w\frac{\partial v}{\partial z} + \frac{uv}{x} = \frac{v}{1+\lambda_1}\frac{\partial^2 v}{\partial z^2}$$

$$+ \frac{v\lambda_2}{1+\lambda_1}\left\{\frac{\partial^3 v}{\partial z^2 \partial t} + u\frac{\partial^3 v}{\partial z^2 \partial x} + \frac{\partial u}{\partial z}\frac{\partial^2 v}{\partial x\partial z} + w\frac{\partial^3 v}{\partial z^3}\right. \tag{3}$$

$$\left. + \frac{\partial w}{\partial z}\frac{\partial^2 v}{\partial z^2}\right\} - \frac{\sigma}{\rho}B^2 v,$$

$$\left(\frac{\partial T}{\partial t} + u\frac{\partial T}{\partial x} + w\frac{\partial T}{\partial z}\right) = \alpha\frac{\partial^2 T}{\partial z^2} + \frac{(\rho c)_p}{(\rho c)_f}\left[D_B C_z T_Z\right.$$

$$\left. + \frac{D_T}{T_\infty}\left(\frac{\partial T}{\partial z}\right)^2\right], \tag{4}$$

$$\frac{\partial C}{\partial t} + u\frac{\partial C}{\partial x} + w\frac{\partial C}{\partial z} = D_B\frac{\partial^2 C}{\partial z^2} - \frac{D_T}{T_\infty}\left(\frac{\partial T}{\partial z}\right)^2, \tag{5}$$

$$\frac{\partial n}{\partial t} + u\frac{\partial n}{\partial x} + w\frac{\partial n}{\partial z} + \frac{bw_c}{(C_w - C_\infty)}\left[\frac{\partial}{\partial z}\left(n\frac{\partial C}{\partial z}\right)\right]$$

$$= D_n\frac{\partial^2 n}{\partial z^2}. \tag{6}$$

The important boundary conditions are as follows:

$$u(x,0,t) = w(x,0,t) = 0,$$

$$v(x,0,t) = \Omega x \sin\alpha^* (1 - st^*)^{-1},$$

$$kT_z(x,0,t) = -v_w,$$

$$\rho D C_z(x,0,t) = -m_w,$$

$$\chi(t,x,0) = \chi_w, \tag{7}$$

$$u(x,\infty,t) = v(x,\infty,t) = 0,$$

$$T(x,\infty,t) = T_\infty,$$

$$C(x,\infty,t) = C_\infty,$$

$$\chi(x,\infty,t) = \chi_\infty.$$

T is the temperature, C is concentration and n represents the concentration of microorganism in the fluid, n_∞ is the density of motile microorganisms in the fluid, γ is the average volume of microorganisms, β is the fluid volume expansion coefficient, and λ_1 is the ratio of relaxation and retardation whereas λ_2 is the retardation time. b is the chemotaxis constant and w_c is maximum cell swimming speed.

Upon application of the following transformations [7]:

$$v_e = \Omega x \sin\alpha^* (1 - st^*)^{-1},$$

$$\eta = \left(\frac{\Omega \sin\alpha^*}{v}\right)^{1/2}(1 - st^*)^{-1/2} z,$$

$$t^* = (\Omega \sin\alpha^*) t,$$

$$u(t,x,z) = -2^{-1}\Omega x \sin\alpha^* (1 - st^*)^{-1} f'(\eta),$$

$$v(t,x,z) = \Omega x \sin\alpha^* (1 - st^*)^{-1} g(\eta),$$

$$w(t,x,z) = (v\Omega \sin\alpha^*)^{1/2}(1 - st^*)^{-1/2} f(\eta),$$

$$T(t,x,z) - T_\infty = (T_0 - T_\infty)\left(\frac{x}{L}\right)(1 - st^*)^{-2}\theta(\eta),$$

$$C(t,x,z) - C_\infty = (C_0 - C_\infty)\left(\frac{x}{L}\right)(1 - st^*)^{-2}\phi(\eta),$$

$$Gr_1 = g\beta\cos\alpha^* (T_0 - T_\infty)\frac{L^3}{v^2},$$

$$Gr_2 = g\beta\cos\alpha^* (C_0 - C_\infty)\frac{L^3}{v^2},$$

$$Re_L = \Omega \sin\alpha^* \frac{L^2}{v},$$

$$\gamma_1 = \frac{Gr_1}{Re_L^2},$$

$$\gamma_2 = \frac{Gr_2}{Re_L^2},$$

$$Nr = \frac{\gamma_2}{\gamma_1},$$

$$P_r = \frac{v}{\alpha},$$

$$S_c = \frac{v}{D},$$

$$A = \lambda_2\Omega \sin\alpha^* (1 - st^*)^{-1}. \tag{8}$$

And then subject to (1) to (6) along with boundary conditions (7) developed a set of five nonlinear differential equations with single variable.

$$\frac{1}{1+\lambda}f''' - ff'' + \frac{1}{2}f'^2 - 2g^2 - 2\gamma_1(\theta - Nr\phi$$

$$- Rb\chi) - s\left(f' + \frac{1}{2}\eta f''\right) + \frac{A}{1+\lambda}\left(\frac{1}{2}f'f''' \right. \tag{9}$$

$$\left. + \frac{1}{2}s\eta f^{iv} - \frac{1}{2}f''^2 + ff^{iv} + 2sf'''\right) - Mf' = 0,$$

$$\frac{1}{1+\lambda}g'' - (fg' - gf') - s\left(g + \frac{1}{2}\eta g'\right)$$

$$- \frac{A}{1+\lambda}\left(2sg'' + \frac{1}{2}s\eta g''' + \frac{1}{2}g''f' - \frac{1}{2}f''g \right. \tag{10}$$

$$\left. + fg'''\right) - Mg = 0,$$

$$\theta'' - \Pr\left[s\left(\frac{1}{2}\eta\theta' + 2\theta\right) + f\theta' - f'\frac{\theta}{2}\right] + Nt\theta'\phi'$$

$$+ Nt\theta'^2 = 0, \tag{11}$$

$$\phi'' - Sc\left[s\left(\frac{1}{2}\eta\phi' + 2\phi\right) + f\phi' - f'\frac{\phi}{2}\right] + \frac{Nt}{Nb}\theta'' = 0, \tag{12}$$

$$\chi'' - \mathrm{Sb}\left[s\left(\frac{1}{2}\eta\chi' + 2\chi\right) + f\chi' - f'\frac{\chi}{2}\right]$$

$$- Pe\left(\phi''\left(\chi + \Omega\right) + \phi'\chi'\right) = 0. \tag{13}$$

Pe, Rb, Nb, Nt, M, Nr, Sb and Sc are bio convection Peclet number, bioconvection Rayleigh number, Brownian motion parameter, thermophoresis parameter, Hartmann number, buoyancy ratio parameter, bioconvection, and Schmidt numbers, respectively.

The dimensionless boundary conditions are

$$f = 0 = f',$$

$$g = 1,$$

$$\theta' = \phi' = -1,$$

$$\chi = 1$$

$$\text{as } \eta \longrightarrow 0,$$

$$f' = 0 = f'', \tag{14}$$

$$g = 0 = g',$$

$$\theta = \phi = 0,$$

$$\chi = 0$$

$$\text{as } \eta \longrightarrow \infty.$$

The coefficients of skin-friction in both x and y –directions are correspondingly specified as

$$C_{fx} = \frac{[2\tau_{xz}]_{z=0}}{\rho\left[\Omega x \sin\alpha^* \left(1 - st^*\right)^{-1}\right]^2}, \tag{15}$$

$$C_{fy} = \frac{[2\tau_{yz}]_{z=0}}{\rho\left[\Omega x \sin\alpha^* \left(1 - st^*\right)^{-1}\right]^2}, \tag{16}$$

or

$$C_{fx}Re_x^{1/2} = \frac{1}{1+\lambda}\left[-f''\right.$$

$$\left. + \frac{A}{2}\left(f'f'' - 3sf'' + 2ff''' + \eta sf'''\right)\right]_{\eta=0},$$

$$C_{fy}Re_x^{1/2} = \frac{1}{1+\lambda}\left[-g'\right. \tag{17}$$

$$\left. - \frac{A}{2}\left(3sg' - f'g' + 2g''f + s\eta g''\right)\right]_{\eta=0}.$$

The Nusselt, Sherwood, and density of motile microorganisms are, respectively, given by

$$NuRe_x^{-1/2} = \frac{1}{\theta(0)},$$

$$ShRe_x^{-1/2} = \frac{1}{\phi(0)}, \tag{18}$$

$$NnRe_x^{-1/2} = -\chi'(0).$$

3. Analytical Solutions by OHAM

The solution of group of mixed nonlinear equations (9) to (13) in series form is computed with the optimal homotopy analysis method (OHAM). The appropriate initial guesses f_0, g_0, θ_0, ϕ_0, and χ_0 are as follows:

$$f_0(\eta) = 0,$$

$$g_0(\eta) = \exp(-\eta),$$

$$\theta_0(\eta) = \exp(-\eta), \tag{19}$$

$$\phi_0(\eta) = \exp(-\eta),$$

$$\chi_0(\eta) = \exp(-\eta).$$

And the linear operators ζ_f, ζ_g, ζ_θ, ζ_ϕ, and ζ_χ for this problem are as follows:

$$\zeta_f(\eta) = f''' - f',$$

$$\zeta_g(\eta) = g'' - g,$$

$$\zeta_\theta(\eta) = \theta'' - \theta, \tag{20}$$

$$\zeta_\phi(\eta) = \phi'' - \phi,$$

$$\zeta_\chi(\eta) = \chi'' - \chi.$$

3.1. Optimal Convergence-Control Parameters. The auxiliary parameters which are involved in the convergence of the homotopic solutions are c_0^f, c_0^g, c_0^θ, c_0^ϕ and c_0^χ. We have engaged the notion of minimization by introducing the residual errors to find out the optimum values of c_0^f, c_0^g, c_0^θ, c_0^ϕ and c_0^χ as introduced by [34].

The Mathematica package BVPh2.0 is used to minimize the average residual error. Three arrays of total optimum convergence control parameters are attained at 2nd, 4th, and 6th iterations.

With 6th iteration optimum convergence-control parameter, singular averaged squared residual errors are achieved and offered in Table 2. Averaged-squared residual errors and total averaged-squared residual errors are reduced by increasing the approximations.

4. Graphical Outcomes and Discussion

The intention of concern segment is to inspect the impacts of various parameters on flow, heat, concentration, and gyrotactic microorganisms. The influence of ratio of relaxation and retardation times λ, Deborah number A, and bioconvection Rayleigh number Rb on the tangential velocity is sketched in Figures 2(a)–2(c). It is depicted that tangential velocity $-f'(\eta)$ has a decreasing behavior for A and Rb but increasing behavior for λ. Similarly, the features of λ, A, and Rb are examined on the azimuthal velocity $g(\eta)$(see Figures 3(a)–3(c)). Here positive values of A and λ result in reduction of azimuthal velocity $g(\eta)$; meanwhile Rb enhances
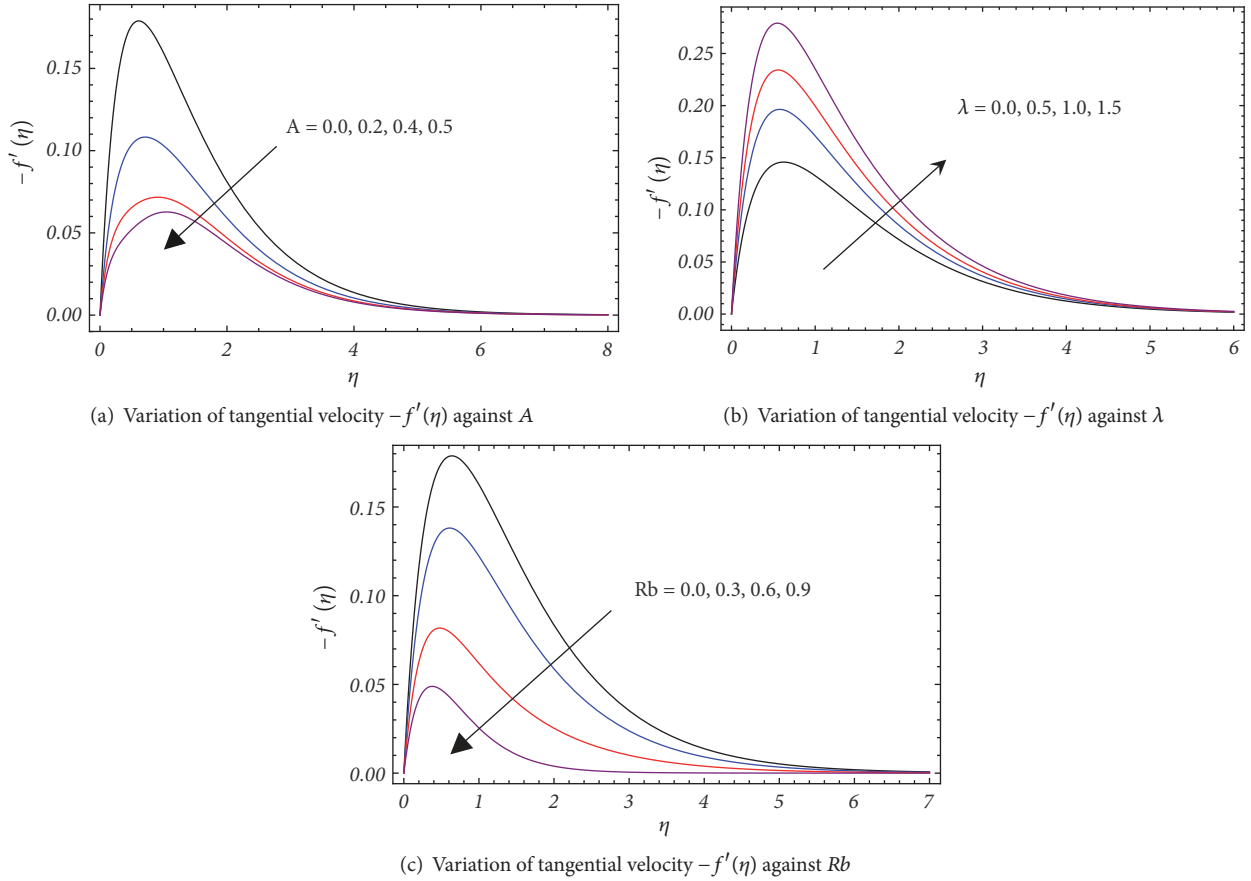
(a) Variation of tangential velocity $-f'(\eta)$ against A

(b) Variation of tangential velocity $-f'(\eta)$ against λ

(c) Variation of tangential velocity $-f'(\eta)$ against Rb

FIGURE 2

TABLE 1: Optimal convergence control parameters and total averaged squared residual errors using *BVPh2.0*.

m	c_0^f	c_0^g	c_0^θ	c_0^ϕ	c_0^χ	E_m^t	CPU TIME[S]
2.0	−1.04	−0.19	−1.06	−1.06	-1.39	1.34×10^{-3}	31.65
4.0	−1.88	−0.42	−0.92	−0.97	-1.49	2.08×10^{-4}	360.27
6.0	−0.90	−0.39	−0.79	−0.89	-1.56	4.92×10^{-5}	12253.3

TABLE 2: Single averaged squared residual errors using optimum values at $m = 6$ from Table 1.

m	E_m^f	E_m^g	E_m^θ	E_m^ϕ	E_m^χ	CPU TIME[S]
6.0	1.18×10^{-5}	5.98×10^{-6}	4.44×10^{-6}	9.82×10^{-6}	1.71×10^{-5}	32.59
12.0	6.50×10^{-7}	1.71×10^{-7}	3.09×10^{-8}	2.90×10^{-7}	7.69×10^{-7}	128.56
18.0	3.17×10^{-7}	4.66×10^{-10}	1.65×10^{-10}	5.27×10^{-10}	5.60×10^{-8}	394.23

the magnitude of boundary layer thickness. Also it is noted that the behavior of $\lambda > 0$ is opposite for $-f'(\eta)$ and $g(\eta)$.

Further, Figures 4(a)–4(c) show that the magnitude of temperature for Nb and Nt is increased and reduced for Pr. Its notable, Brownian motion of nanoparticles offers a main role in nanofluids to augment the heat transfer. Therefore, it can be encouraged that nanofluids and magnetic field intensity create variation in the fluid's temperature and as such, the use of nanofluids in a magnetic field will be noteworthy in the cooling and heating processes. Additional heat is produced by the contact of nanoparticles and the base fluid because

of Brownian motion and thermophoresis. So, the thermal boundary layer develops thicker and the effect is so noticeable that strong temperature exceeds are eminent in the vicinity of the cone for elevating Nb and Nt. And intense particles are dragged from hot surface to the cold area for thermophoresis phenomena. Thus the temperature of the fluid rises. Actually for escalation in Pr, the thermal diffusivity shrinks which significantly decays the temperature. On the other hand, the effects of Brownian motion parameter Nb, thermophoresis parameter Nt, and Schmidt number Sc on concentration are also discussed in Figures 5(a)–5(c). It is portrayed that
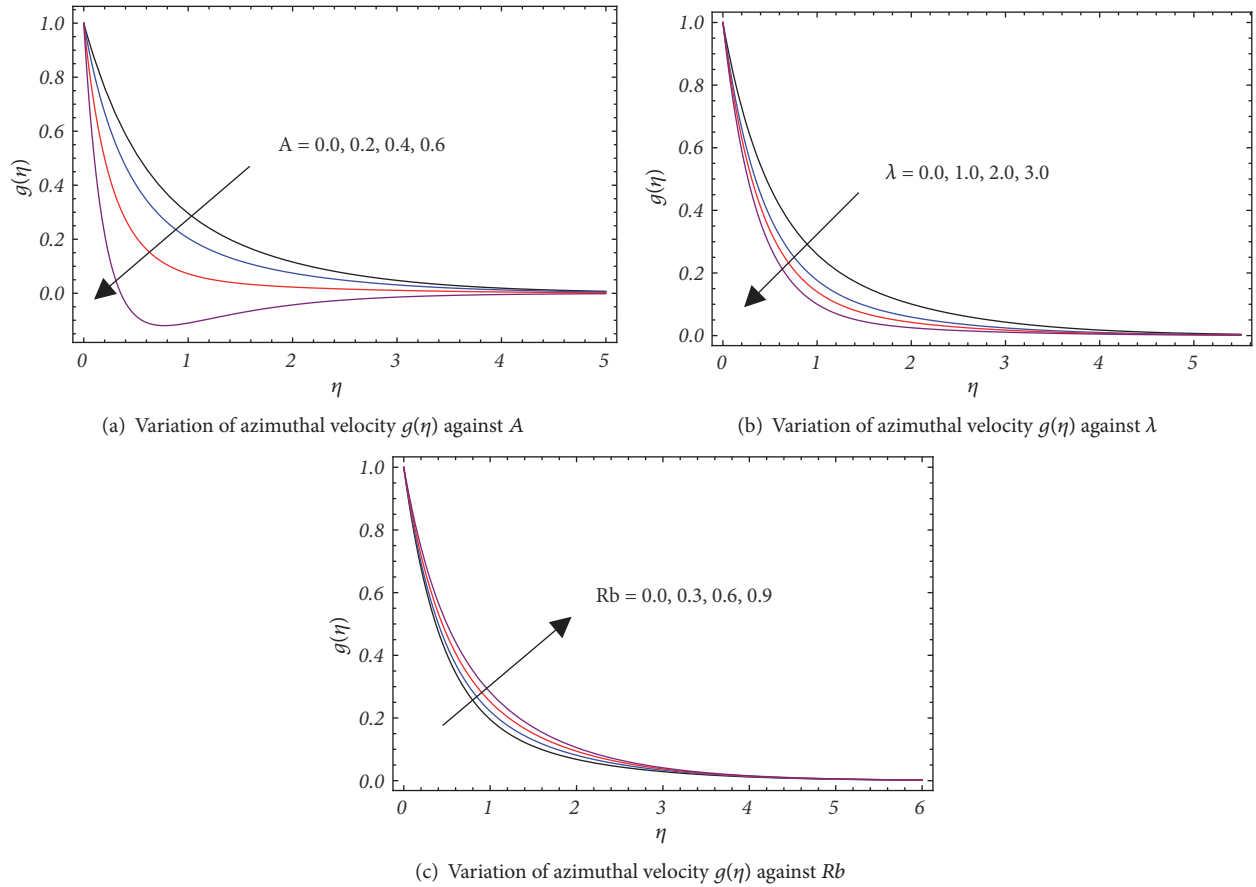
(a) Variation of azimuthal velocity $g(\eta)$ against A

(b) Variation of azimuthal velocity $g(\eta)$ against λ

(c) Variation of azimuthal velocity $g(\eta)$ against Rb

FIGURE 3

TABLE 3: Comparative results for important physical quantities for special case $Pe = Sb = A = Rb = \lambda = 0$.

	Present results		Numerical results [7]	
M	$C_{fx}Re_x^{1/2}$	$C_{fy}Re_x^{1/2}$	$C_{fy}Re_x^{1/2}$	$C_{fy}Re_x^{1/2}$
0.0	1.0205	0.6154	1.0207	0.6159
			1.021*	0.616*
0.5	0.7735	0.8485	0.7730	0.8488
			0.770*	0.849*
1.0	0.6197	1.0695	0.6194	1.0692
			0.619*	1.069*
2.0	0.4617	1.4411	0.4613	1.4418
			0.461*	1.442*
3.0	0.3817	1.7476	0.3813	1.7477
			0.381*	1.748*

*Sparrow and Cess [10].

the concentration of fluid particles reduces in magnitude for Nb and Sc, while the magnitude goes higher for Nt. Schmidt number shows converse relation for coefficient of Brownian diffusion. Greater values of Sc are a source of smaller Brownian diffusion coefficient which is responsible to decrease the concentration field.

Figures 6(a) and 6(b) demonstrate the impact of gyrotactic microorganism parameters on density of motile microorganism $\chi(\eta)$. It is explored that the density of motile microorganism is a decreasing function of microorganism Peclet number Pe and bioconvection Schmidt number Sb. In fact Peclet number is proportion of extreme cell swimming speed to diffusivity of microorganisms as escalation in Pe enhances cell swimming speed so rise in Peclet number shrinks the density of motile microorganisms.
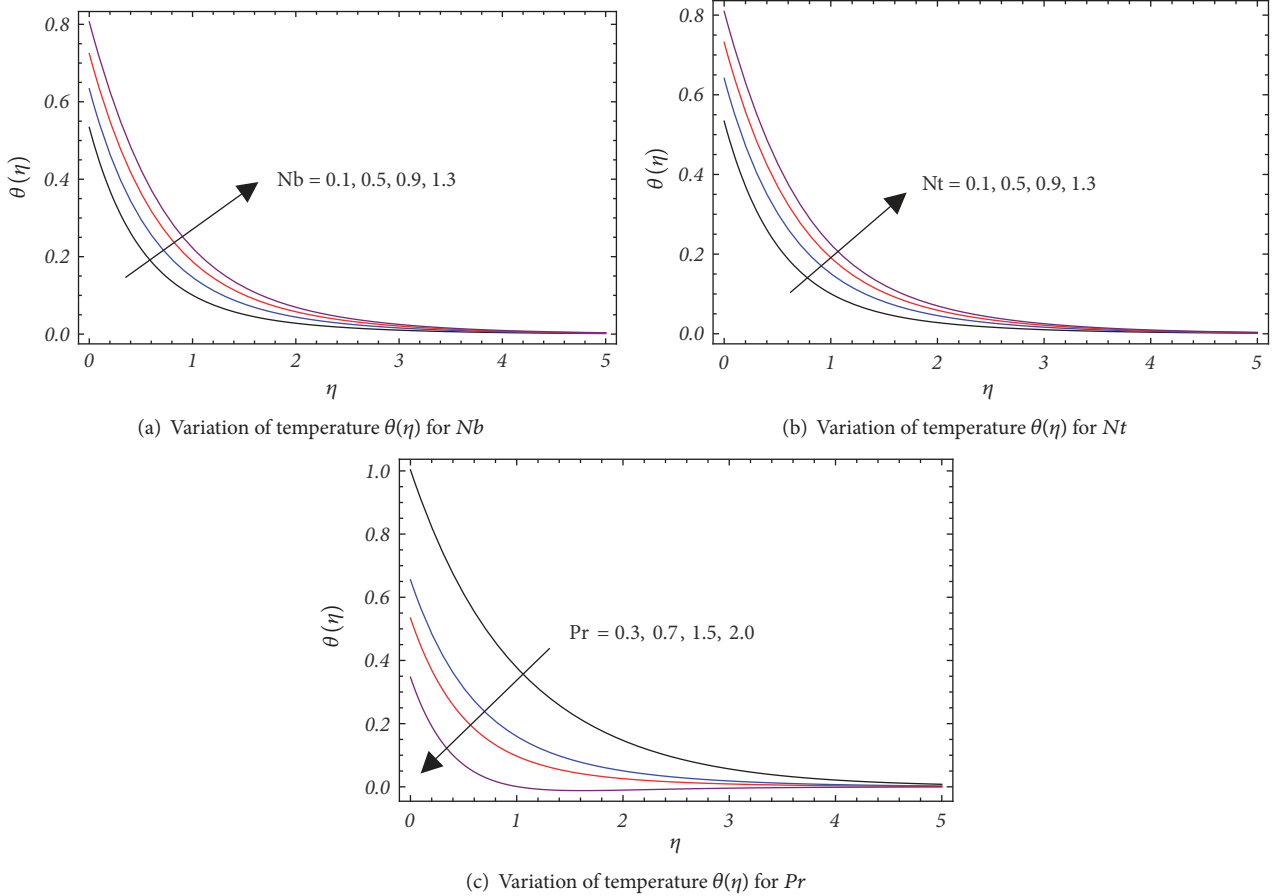
(a) Variation of temperature $\theta(\eta)$ for Nb

(b) Variation of temperature $\theta(\eta)$ for Nt

(c) Variation of temperature $\theta(\eta)$ for Pr

FIGURE 4

TABLE 4: Surface skin friction coefficients for some significant parameters.

λ	M	γ_1	Nr	$C_{fx}Re_x^{1/2}$	$C_{fy}Re_x^{1/2}$
0.5				3.06172	0.58831
1.0				2.92640	0.52921
1.5				1.92763	0.48527
	0.5			4.4517	1.2593
	1.0			4.3485	2.3509
	1.5			4.2310	3.3476
		1.0		2.7583	0.7576
		1.5		3.5482	0.8572
		2.0		4.2382	0.9438
			0.5	3.4620	0.5072
			1.0	4.3947	0.6373
			1.5	5.1926	0.7493

The influences of Pe and Sb on $-\chi'(0)$ are plotted in Figure 7. It is very clear from the figure that $-\chi'(0)$ has a direct relation with both Pe and Sb for accelerating flow (i.e., $s > 0$). On the other hand when flow is retarding the aptitude of $-\chi'(0)$ is opposite for Pe and Sb. This determines that bioconvection Schmidt number creates huge resistance to the motion of the fluid. Thus, Sb is much more effective in the boundary layer region. This is predictable since the viscous diffusion rate escalates due to a rise in Sb. which results in significant reduction in $-\chi'(0)$.

In addition, to verify the stability of present results, comparison in Table 3 is computed in the deficiency of buoyancy force, Peclet number, and bioconvection Schmidt number with the results given by Sparrow and Cess [10]. The outcomes are seen to be in decent compatible order with each other.
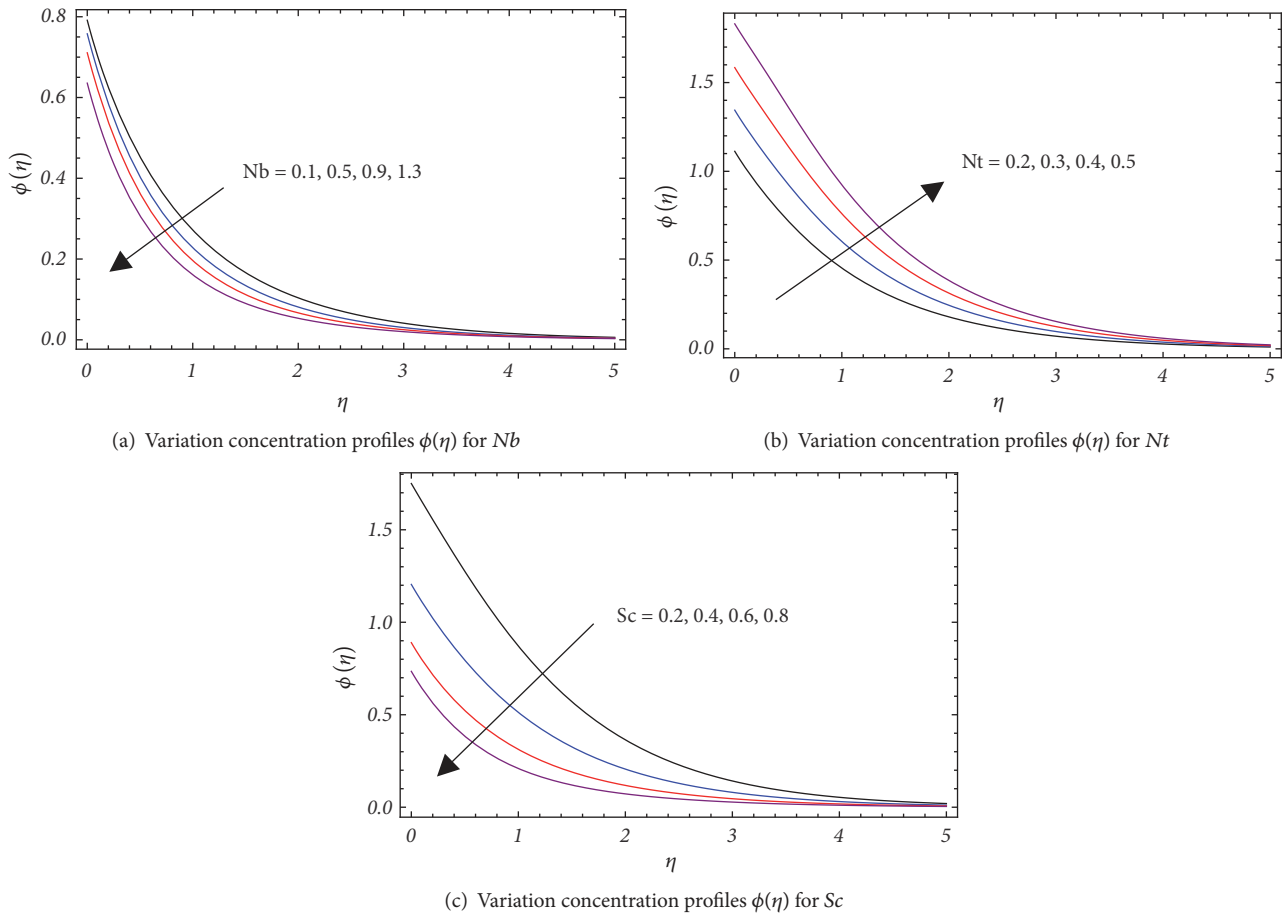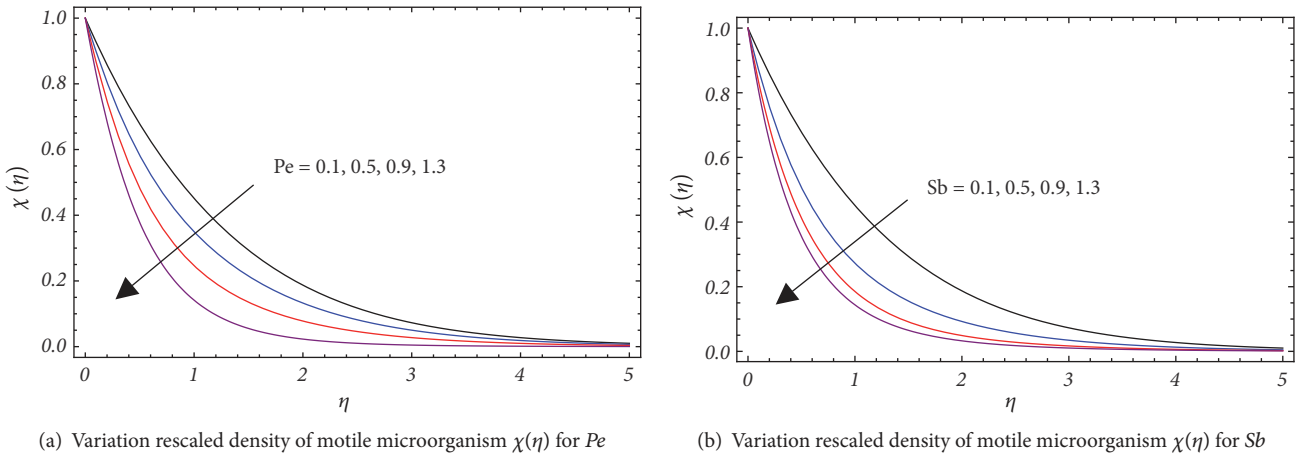
(a) Variation concentration profiles $\phi(\eta)$ for Nb

(b) Variation concentration profiles $\phi(\eta)$ for Nt

(c) Variation concentration profiles $\phi(\eta)$ for Sc

FIGURE 5

(a) Variation rescaled density of motile microorganism $\chi(\eta)$ for Pe

(b) Variation rescaled density of motile microorganism $\chi(\eta)$ for Sb

FIGURE 6

Table 4 is prepared for values of skin friction coefficients against ratio of relaxation and retardation times λ, magnetic parameter M, buoyancy parameter γ_1, and ratio of buoyancy forces N. It is obvious that tangential skin friction coefficient rises with larger γ_1 and N, but decreases with both λ and M. Besides this, azimuthal skin friction coefficient is directly proportional to all these pertinent parameters expect λ. Actually,

we can say that closing the walls of cone the temperature of the wall is more prominent than the temperature of the fluid which eventually rises Gr_2 as compared to Gr_1; therefore greater N offers the larger skin friction values.

The behavior of Pr, Sc, and N on heat and mass transfer rate coefficient is deliberated in Table 5. It is found that Pr and N boost the heat transfer rate coefficient while the variation is

TABLE 5: Variation of local Nusselt and Sherwood numbers for certain noteworthy parameters.

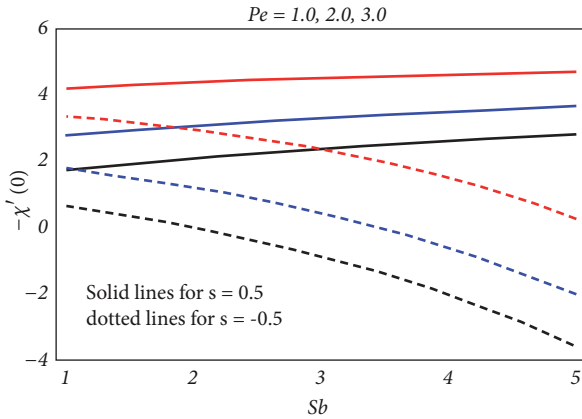| Pr	Sc	Nr	$NuRe_x^{-1/2}$	$ShRe_x^{-1/2}$
3.0			0.8450	0.8495
7.0			1.1035	0.8492
12.0			1.2431	0.8485
	1.0		0.6684	0.8790
	2.0		0.6676	1.1570
	3.0		0.6667	1.7639
		0.5	0.6184	0.8703
		1.0	0.6354	0.8623
		1.5	0.6512	0.8576

FIGURE 7: Variation of reduced density number of the motile microorganisms $-\chi'(0)$ with bioconvection parameters.

opposite for Sc. Also the mass transfer rate coefficient shows an increasing aptitude for changed values of N and Sc. On the contrary, Pr reduces the magnitude of mass transfer rate coefficient.

5. Conclusions

This investigation gives analytical solutions of flow, heat, and mass transfer in MHD Jeffrey nanofluid on a rotating cone with motile microorganism. Based on the calculated outcomes, the subsequent summary is reached at the following:

(i) The tangential skin friction coefficient varies as an inverse function of λ.

(ii) Rescaled density of the motile microorganisms shrinks with both Pe and Sb.

(iii) The impression of M is to decline the major skin friction while increasing the minor skin friction.

(iv) The effect of Nb is opposite for temperature and concentration fields.

(v) Growing values of Pe and Sb augment the reduced density number of the motile microorganisms for positive s.

(vi) This study is pertinent in aerospace manufacturing for design and improvement of apparatus.

Nomenclature

Pe: Bio convection Peclet number
Rb: Bioconvection Rayleigh number
Nb: Brownian motion parameter
Nt: Thermophoresis parameter
M: Hartmann number
C_{fx}: Local skin friction coefficient
F: Dimensionless stream function
N: Concentration of microorganism in the fluid
Nr: Buoyancy ratio parameter
λ_1: Ratio of relaxation and retardation
λ_2: Retardation time
Sb: Bioconvection Schmidt number
SC: Schmidt number
n_∞: Density of motile microorganisms
γ: Average volume of microorganisms
b: Chemotaxis constant
w_c: Maximum cell swimming speed
Nu_x: Local Nusselt number
Pr: Prandtl number
Re: Local Reynolds number
T: Fluid temperature
T_w: Temperature at the wall
T_∞: Ambient temperature of the fluid
U: Velocity component in the x-direction
U_0: Characteristic velocity
u_w: Stretching sheet velocity
V: Velocity component in the y-direction
z: Streamwise coordinate
Y: Cross-stream coordinate.

Greek Symbols

α: Thermal diffusivity
β: Volumetric coefficient of the thermal expansion
θ: Dimensionless temperature
ρ: Fluid density
η: Similarity independent variable
ψ: Stream function
Ω: Angular velocity of the cone.

Subscripts

W: Quantities at wall
∞: Quantities far away from the surface.

Data Availability

No data were used to support this study.

Conflicts of Interest

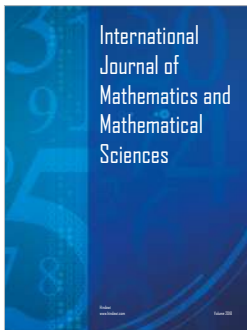The authors declare that they have no conflicts of interest.

Acknowledgments

References

[1] R. Ellahi, "Effects of the slip boundary condition on non-Newtonian flows in a channel," *Communications in Nonlinear Science and Numerical Simulation*, vol. 14, no. 4, pp. 1377–1384, 2009.

[2] A. Hussain, R. Zetoon, S. Ali, and S. Nadeem, "Magnetically driven flow of pseudoplastic fluid across a sensor surface," *Journal of the Brazilian Society of Mechanical Sciences and Engineering*, vol. 41, no. 4, p. 185, 2019.

[3] M. Abd El-Aziz and A. A. Afify, "Influences of slip velocity and induced magnetic field on mhd stagnation-point flow and heat transfer of casson fluid over a stretching sheet," *Mathematical Problems in Engineering*, vol. 2018, Article ID 9402836, 11 pages, 2018.

[4] M. Qasim, M. I. Afridi, A. Wakif, and S. Saleem, "Influence of variable transport properties on nonlinear radioactive jeffrey fluid flow over a disk: utilization of generalized differential quadrature method," *Arabian Journal for Science and Engineering*, 2019.

[5] R. Mehmood, S. Nadeem, S. Saleem, and N. S. Akbar, "Flow and heat transfer analysis of Jeffery nano fluid impinging obliquely over a stretched plate," *Journal of the Taiwan Institute of Chemical Engineers*, vol. 74, pp. 49–58, 2017.

[6] R. G. Hering and R. J. Grosh, "Laminar combined convection from a rotating cone," *Journal of Heat Transfer*, vol. 85, no. 1, pp. 29–34, 1963.

[7] D. Anilkumar and S. Roy, "Unsteady mixed convection flow on a rotating cone in a rotating fluid," *Applied Mathematics and Computation*, vol. 155, no. 2, pp. 545–561, 2004.

[8] S. Nadeem and S. Saleem, "Analytical treatment of unsteady mixed convection MHD flow on a rotating cone in a rotating frame," *Journal of the Taiwan Institute of Chemical Engineers*, vol. 44, no. 4, pp. 596–604, 2013.

[9] C. S. K. Raju, N. Sandeep, and A. Malvandi, "Free convective heat and mass transfer of MHD non-Newtonian nanofluids over a cone in the presence of non-uniform heat source/sink," *Journal of Molecular Liquids*, vol. 221, pp. 108–115, 2016.

[10] E. M. Sparrow and R. D. Cess, "Magnetohydrodynamic flow and heat transfer about a rotating disk," *Journal of Applied Mechanics*, vol. 29, pp. 181–187, 1962.

[11] S. Saleem, M. M. Al-Qarni, S. Nadeem, and N. Sandeep, "Convective heat and mass transfer in magneto jeffrey fluid flow on a rotating cone with heat source and chemical reaction," *Communications in Theoretical Physics*, vol. 70, no. 5, pp. 534–540, 2018.

[12] S. Saleem, H. Firdous, S. Nadeem, and A. U. Khan, "Convective heat and mass transfer in magneto walter's b nanofluid flow induced by a rotating cone," *Arabian Journal for Science and Engineering*, vol. 44, no. 2, pp. 1515–1523, 2019.

[13] S. U. S. Choi, "Enhancing thermal conductivity of fluids with nanoparticles," *Developments and Applications of Non-Newtonian Flows*, vol. 66, pp. 99–105, 1995.

[14] J. Buongiorno, "Convective transport in nanofluids," *ASME Journal of Heat Transfer*, vol. 128, no. 3, pp. 240–250, 2006.

[15] S. Kakaç and A. Pramuanjaroenkij, "Review of convective heat transfer enhancement with nanofluids," *International Journal of Heat and Mass Transfer*, vol. 52, no. 13-14, pp. 3187–3196, 2009.

[16] M. Sheikholeslami, A. Ghasemi, Z. Li, A. Shafee, and S. Saleem, "Influence of CuO nanoparticles on heat transfer behavior of PCM in solidification process considering radiative source term," *International Journal of Heat and Mass Transfer*, vol. 126, pp. 1252–1264, 2018.

[17] M. Sheikholeslami, M. Jafaryar, S. Saleem, Z. Li, A. Shafee, and Y. Jiang, "Nanofluid heat transfer augmentation and exergy loss inside a pipe equipped with innovative turbulators," *International Journal of Heat and Mass Transfer*, vol. 126, pp. 156–163, 2018.

[18] M. A. Sadiq, A. U. Khan, S. Saleem, and S. Nadeem, "Numerical simulation of oscillatory oblique stagnation point flow of a magneto micropolar nanofluid," *RSC Advances*, vol. 9, no. 9, pp. 4751–4764, 2019.

[19] A. Hussain, L. Sarwar, S. Akbar, M. Y. Malik, and S. Ghafoor, "Model for MHD viscoelastic nanofluid flow with prominence effects of radiation," *Heat Transfer - Asian Research*, 2018.

[20] M. Sheikholeslami, S. Saleem, A. Shafee et al., "Mesoscopic investigation for alumina nanofluid heat transfer in permeable medium influenced by Lorentz forces," *Computer Methods Applied Mechanics and Engineering*, vol. 349, pp. 839–858, 2019.

[21] S. Saleem, S. Nadeem, M. M. Rashidi, and C. S. Raju, "An optimal analysis of radiated nanomaterial flow with viscous dissipation and heat source," *Microsystem Technologies*, vol. 25, no. 2, pp. 683–689, 2019.

[22] M. M. Rashidi, B. Rostami, N. Freidoonimehr, and S. Abbasbandy, "Free convective heat and mass transfer for MHD fluid flow over a permeable vertical stretching sheet in the presence of the radiation and buoyancy effects," *Ain Shams Engineering Journal*, vol. 5, no. 3, pp. 901–912, 2014.

[23] R. Ellahi, "The effects of MHD and temperature dependent viscosity on the flow of non-Newtonian nanofluid in a pipe: analytical solutions," *Applied Mathematical Modelling*, vol. 37, no. 3, pp. 1451–1467, 2013.

[24] M. Awais, M. Y. Malik, S. Bilal, T. Salahuddin, and A. Hussain, "Magnetohydrodynamic (MHD) flow of Sisko fluid near the axisymmetric stagnation point towards a stretching cylinder," *Results in Physics*, vol. 7, pp. 49–56, 2017.

[25] N. A. Hill and T. J. Pedley, "Bioconvection," *Japan Society of Fluid Mechanics. Fluid Dynamics Research*, vol. 37, no. 1-2, pp. 1–20, 2005.

[26] S. E. Ahmed, A. M. Aly, and M. A. Mansour, "MHD mixed bioconvection stagnation point flow of nanofluids towards a stretching surface," *Journal of Nanofluids*, vol. 4, no. 4, pp. 528–535, 2015.

[27] A. V. Kuznetsov, "The onset of nanofluid bioconvection in a suspension containing both nanoparticles and gyrotactic microorganisms," *International Communications in Heat and Mass Transfer*, vol. 37, no. 10, pp. 1421–1425, 2010.

[28] W. A. Khan and O. D. Makinde, "MHD nanofluid bioconvection due to gyrotactic microorganisms over a convectively heat stretching sheet," *International Journal of Thermal Sciences*, vol. 81, no. 1, pp. 118–124, 2014.

[29] W. A. Khan, O. D. Makinde, and Z. H. Khan, "MHD boundary layer flow of a nanofluid containing gyrotactic microorganisms past a vertical plate with Navier slip," *International Journal of Heat and Mass Transfer*, vol. 74, pp. 285–291, 2014.

[30] C. S. K. Raju and N. Sandeep, "Dual solutions for unsteady heat and mass transfer in Bio-convection flow towards a rotating cone/plate in a rotating fluid," *International Journal of Engineering Research in Africa*, vol. 20, pp. 161–176, 2016.

[31] K. Zaimi, A. Ishak, and I. Pop, "Stagnation-point flow toward a stretching/shrinking sheet in a nanofluid containing both nanoparticles and gyrotactic microorganisms," *Journal of Heat Transfer*, vol. 136, no. 4, pp. 1–9, 2014.

[32] S. Siddiqa, Gul-e-Hina, N. Begum, S. Saleem, M. A. Hossain, and R. S. Reddy Gorla, "Numerical solutions of nanofluid bioconvection due to gyrotactic microorganisms along a vertical wavy cone," *International Journal of Heat and Mass Transfer*, vol. 101, pp. 608–613, 2016.

[33] O. D. Makinde and I. L. Animasaun, "Bioconvection in MHD nanofluid flow with nonlinear thermal radiation and quartic autocatalysis chemical reaction past an upper surface of a paraboloid of revolution," *International Journal of Thermal Sciences*, vol. 109, pp. 159–171, 2016.

[34] S. Liao, "Beyond Perturbation: a review on the homotopy analysis method and its applications," *Advance in Mechanics*, vol. 153, pp. 1–34, 2008.

[35] S. Liao, "An optimal homotopy-analysis approach for strongly nonlinear differential equations," *Communications in Nonlinear Science and Numerical Simulation*, vol. 15, no. 8, pp. 2003–2016, 2010.

[36] S. Nadeem, A. Hussain, and M. Khan, "HAM solutions for boundary layer flow in the region of the stagnation point towards a stretching sheet," *Communications in Nonlinear Science and Numerical Simulation*, vol. 15, no. 3, pp. 475–481, 2010.

[37] M. M. Rashidi, A. M. Siddiqui, and M. Asadi, "Application of homotopy analysis method to the unsteady squeezing flow of a second-grade fluid between circular plates," *Mathematical Problems in Engineering*, vol. 2010, Article ID 706840, 18 pages, 2010.

[38] M. Y. Malik, A. Hussain, and S. Nadeem, "Boundary layer flow of an Eyring-Powell model fluid due to a stretching cylinder with variable viscosity," *Scientia Iranica*, vol. 20, no. 2, pp. 313–321, 2013.

[39] M. Awais, S. Saleem, T. Hayat, and S. Irum, "Hydromagnetic couple-stress nanofluid flow over a moving convective wall: OHAM analysis," *Acta Astronautica*, vol. 129, pp. 271–276, 2016.

[40] S. Saleem, M. Awais, S. Nadeem, N. Sandeep, and M. T. Mustafa, "Theoretical analysis of upper-convected Maxwell fluid flow with Cattaneo–Christov heat flux model," *Chinese Journal of Physics*, vol. 55, no. 4, pp. 1615–1625, 2017.